Supplementary Information (SI) for Chemical Communications.

Supporting Information

A cluster-scale CuFe heteroatom ensemble with a multisite interface reinforces electronic interaction to boost ambient ammonia electrosynthesis

Fengchun Zhou,[a] *Sisi Liu,**[a] *Xiaolei Yuan,*[a] *Weiyi Shen,*[a] *Wenjun Shi,*[a] *Kaiwen Xiao,*[a] *Yanqi Li,*[a] *Chenglin Yan,*[b] *and Tao Qian**[a]

[a]School of Chemistry and Chemical Engineering, Nantong University, Nantong 226019, China.
[b]School of Petrochemical Engineering, Changzhou University, Changzhou 213164, China.

Experimental Section

Reagents. Pyrrole (C_4H_5N, 98%) and salicylic acid ($C_7H_6O_3$, 99.5%) were purchased from Sigma-Aldrich. Ferrous chloride tetrahydrate ($FeCl_2 \cdot 4H_2O$, ≥99.0%), hydrogen peroxide solution (H_2O_2, 30%), sodium chloride (NaCl, ≥99.5%), zinc chloride ($ZnCl_2$, ≥98%), copper chloride ($CuCl_2$, ≥99.99%), potassium hydroxide (KOH, ≥99.99%), potassium nitrate (KNO_3, ≥99.99%), sodium citrate dehydrate ($C_6H_5Na_3O_7 \cdot 2H_2O$, 99.0%), sodium hypochlorite solution (NaClO, available chlorine ≥5.0%), sodium nitroferricyanide dihydrate ($C_5FeN_6Na_2O \cdot 2H_2O$, 99.0%), sodium hydroxide (NaOH, 96%), ammonium chloride (NH_4Cl, 99.5%), and *p*-dimethylaminobenzaldehyde ($C_9H_{11}NO$, 99%) were purchased from Aladdin Ltd (China). Hydrochloric acid (HCl, 36.0-38.0%), ethyl alcohol (C_2H_5OH, 75%), hydrazine monohydrate ($N_2H_4 \cdot H_2O$, ≥85.0%), and sulfuric acid (H_2SO_4, 95.0-98.0%) were purchased from Sinopharm Chemical Reagent Co., Ltd. Nafion solution (5 wt.%) was purchased from Alfa Aesar. All the reagents were used without further purification.

Preparation of catalysts. To prepare Fe_{SC}/NC, pyrrole was first dispersed in deionized water. Excess ferrous chloride and hydrogen peroxide were added and stirred for several hours to obtain a bright yellow solution. Then, sodium chloride and zinc chloride were dissolved in the solution to serve as templates. A brown solid material was acquired through freeze-drying. The obtained product was grinded and carbonized at 800 °C under Ar protection for 2 h. After acid pickling and sufficiently washing with water and ethanol, the final products were obtained and denoted as Fe_{SC}/NC. The catalysts were dried in a vacumm at 60 °C before use. The synthesis of $CuFe_{SC}$/NC was similar to that of Fe_{SC}/NC, except that additional copper chloride was added in the solution along with sodium chloride and zinc chloride templates.

Physical characterizations. The iron and copper content of the catalysts were obtained through inductively coupled plasma atomic emission spectroscopy (ICP-OES, Varian-710ES, America). The morphology and microstructure of catalysts were studied via a field emission scanning electron microscopy (FESEM, SU8010, Japan) at an accelerating voltage of 10 kV, and aberration-corrected high-angle annular dark-field scanning transmission electron microscopy (AC HAADF STEM, Titan Themis Cubed G2 300, America). X-ray diffraction (XRD) patterns were acquired on a Bruker D8

Advance (Germany) with Cu Kα radiation of wavelength 0.154 nm to detect the crystallization. The Raman spectroscopy was recorded by a Horiba Jobin Yvon HR evolution system at a wavelength of 532 nm. Surface elemental analysis was carried out on X-ray photoelectron spectrometer (XPS, Thermo Fisher Escalab 250Xi, America). The ultraviolet-visible (UV-vis) absorption spectra were acquired on a UV-2600i spectrophotometer (SHIMADZU, Japan).

Electrochemical measurements. Electrochemical NO_3RR measurements were performed in a gas-tight H-type cell, which has an ion-exchange membrane (Nafion 117) to separate the cathode and anode chambers. Before measurements, the Nafion 117 membrane was pretreated by successive heating in H_2O_2 (5%), ultrapure water, and H_2SO_4 (5%), respectively. To prepare cathode, 1 mg of catalyst and 20 μL of Nafion solution (5 wt.%) were dispersed in 980 μL ethanol ultrasonically for at least 1 h to obtain a homogeneous ink. Then, 50 μL of catalyst ink was coated on carbon paper with area of 1×1 cm^2 and dried at room temperature. Pt wire was used as the counter electrode, and Ag/AgCl (4 M KCl) was used as reference electrode. Both the cathode and anode chamber contained 25 mL of 0.1 M KOH + 0.5 M KNO_3 electrolyte. Before the measurement, the electrolyte was saturated by Ar gas through purging for 30 minutes. All potentials were corrected to the RHE scale using the formula $E_{RHE} = E_{Ag/AgCl} + 0.0591 \times pH + 0.197$. The linear sweep voltammetry (LSV) tests were tested at a rate of 10 mV s^{-1}. The potentiostatic tests were measured at different potentials including, –0.8, –0.9, –1.0, –1.1, and –1.2 V vs. RHE for 1 h. The durability tests were conducted at –0.9 V vs. RHE. The electrolyte was collected every 1 h for ammonia quantification, and the chronoamperometric measurements were then carried out at the same conditions using the fresh electrolyte. After each electrochemical reduction reaction cycle, the electrolyte was collected and analysed by colorimetric methods.

Determination of ammonia. The concentration of NH_3 in the electrolyte was determined by the indophenol blue method. Specifically, 0.1 mL of the electrolyte after electrochemical measurement was taken out and diluted to 10 mL. Then, 2 mL of the diluted solution was mixed with 2 mL of 1 M NaOH solution containing 5 wt% sodium citrate and 5 wt% salicylic acid. Next, 1 mL of 0.05 M sodium hypochlorite solution and 0.2 mL of 1 wt% sodium nitroferricyanide were successively added into the solution. The UV-vis absorption spectrum of the solution was measured after standing in the dark for 2 h. The concentration of indophenol blue was measured using the absorbance at the wavelength of 655 nm. The concentration-absorbance curve was calibrated using standard ammonium chloride at a series of given concentrations in 0.1 M KOH solutions.

Determination of hydrazine. The produced hydrazine in the electrolyte was determined using the Watt and Chrisp method. The chromogenic reagent was prepared by mixing ethanol (300 mL), concentrated HCl (30 mL), and para-(dimethylamino) benzaldehyde (5.99 g). 5 mL of electrolyte after electrocatalytic test was taken out, and 5 mL of the color agent was added into the electrolyte. After standing for 10 min in dark, its absorbance was measured at a wavelength of 455nm. The concentration-absorbance curves were obtained using standard hydrazine monohydrate at a series of given concentrations in 0.1 M KOH solutions.

Yield rate and Faradaic efficiency. The yield rate and Faradaic efficiency of NH_3 were calculated as the following formula:

$$\text{Yield rate } (NH_3) = [c(NH_3) \times V] / (t \times m) \tag{1}$$

$$\text{Faradaic efficiency } (NH_3) = [8F \times c(NH_3) \times V] / (17 \times Q) \tag{2}$$

where $c(NH_3)$ is the measured NH_3 concentration, V is the volume of the electrolyte, t is the reduction time (1 h), m is the loading mass of the catalysts, F is the Faradaic constant (96,485 C mol^{-1}), Q is the total charge passed through the electrode.

Computational method and model. The Fe_{SC}/NC and $CuFe_{SC}$/NC models were built, where the vacuum space along the z direction is set to be 20 Å, which is enough to avoid interaction between the two neighboring configurations. All atom layers and adsorbed intermediates were relaxed adequately to remove the internal stress of systems. The first principles calculations in the framework of density functional theory were carried out based on the Cambridge Sequential Total Energy Package known as CASTEP. The exchange-correlation functional under the generalized gradient approximation (GGA) with norm-conserving pseudopotentials and Perdew-Burke-Ernzerhof functional was adopted to describe the electron–electron interaction. An energy cutoff of 750 eV was used and a k-point sampling set of 5 × 5 × 1 were tested to be converged. A force tolerance of 0.01 eV $Å^{-1}$, energy tolerance of 5.0×10^{-7} eV per atom and maximum displacement of 5.0×10^{-4} Å were considered.

Adsorption energy ΔE of intermediates A on the surface of substrates was defined as:

$$\Delta E_{ads} = \mathrm{E}_{*\mathrm{A}} - (E_{*} + E_{\mathrm{A}}) \tag{3}$$

where *A and * denoted the adsorption of intermediates A on substrates and the bare substrates, E_{A} denoted the energy of A.

Free energy change ΔG of the reaction was calculated as the difference between the free energies of the initial and final states as shown below:

$$\Delta G = \Delta E_{ads} + \Delta \mathrm{ZPE} - T\Delta \mathrm{S} \tag{4}$$

where ΔZPE is the change of zero point energy; T and ΔS denote the temperature and the change of entropy, respectively.

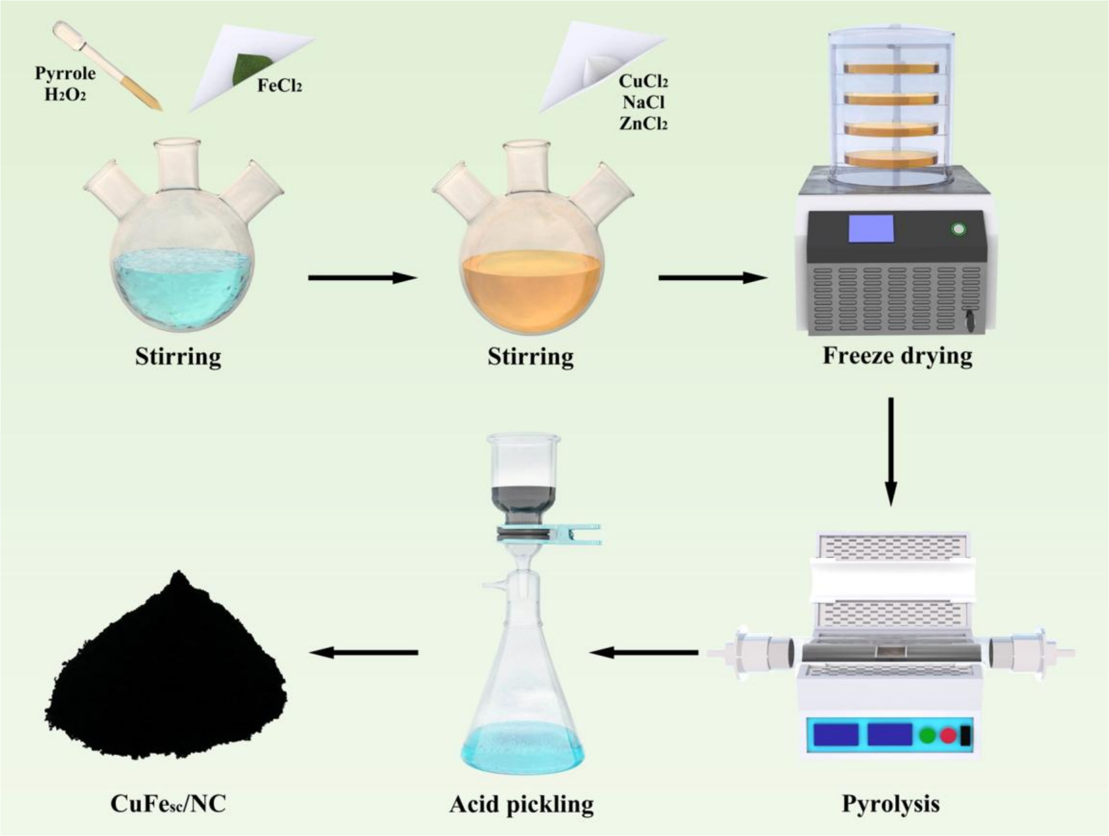

Figure S1. A schematic illustration for the synthesis route of $CuFe_{SC}/NC$.

Table S1. Metal composition content obtained from inductively coupled plasma optical emission spectrometry (ICP-OES).

Samples	Cu wt.%	Fe wt.%
CuFe$_{SC}$-NC	2.49	3.75
Fe$_{SC}$-NC	-	5.84

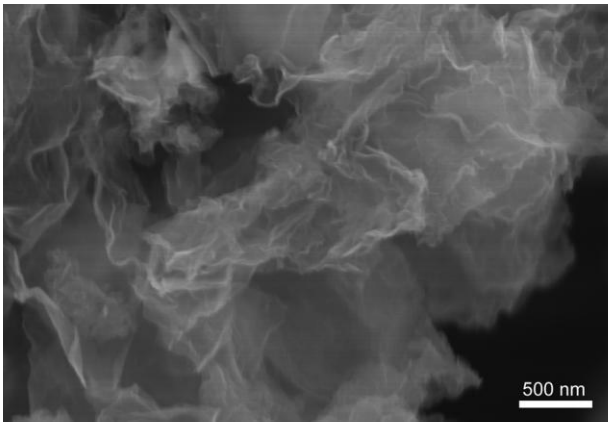

Figure S2. SEM image of $CuFe_{SC}$/NC.

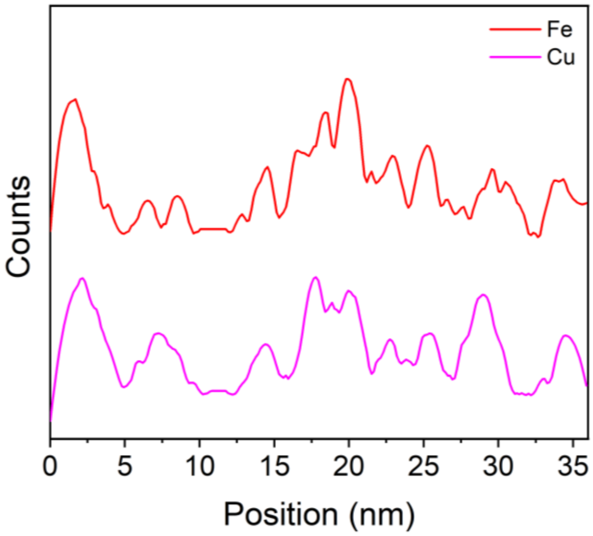

Figure S3. EDS line scan profiles of Cu and Fe signal recorded from the red line in Fig. 1c.

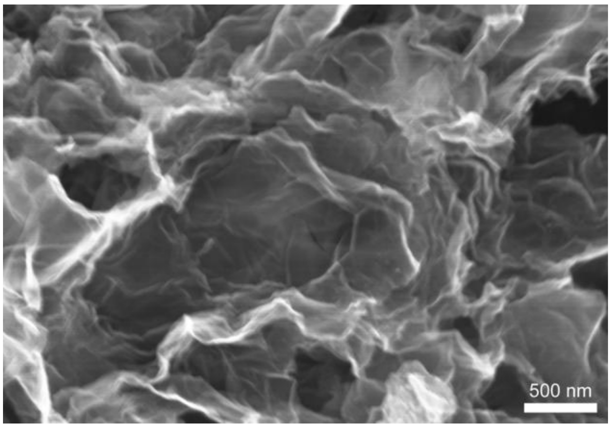

Figure S4. SEM image of Fe_{SC}/NC.

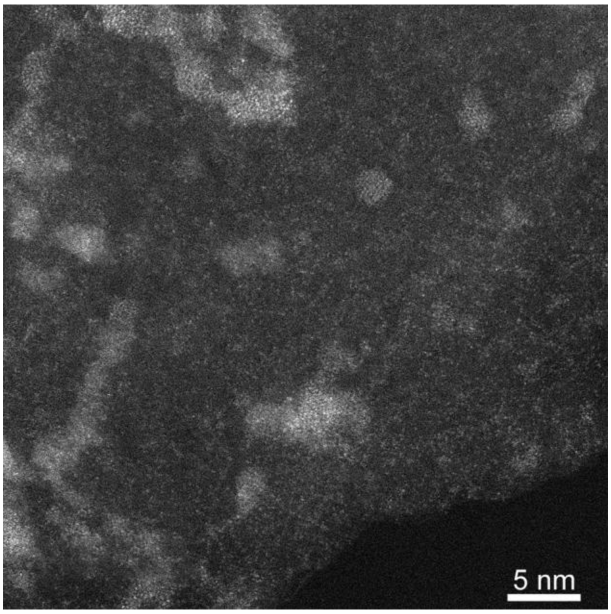

Figure S5. AC-HAADF-STEM image of Fe_{SC}/NC.

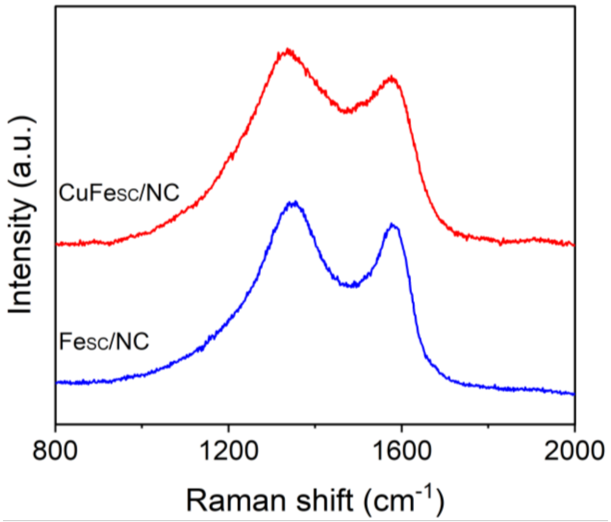

Figure S6. Raman spectra of $CuFe_{SC}$/NC and Fe_{SC}/NC.

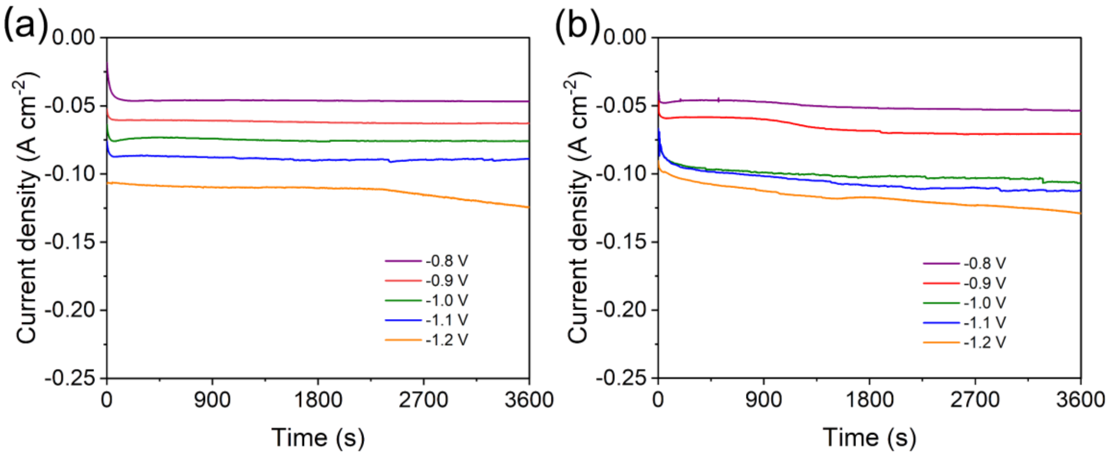

Figure S7. Chronoamperometry results of (a) Fe_{SC}/NC and (b) $CuFe_{SC}$/NC at different applied potentials obtained in 0.1 M KOH with 0.5 M KNO_3.

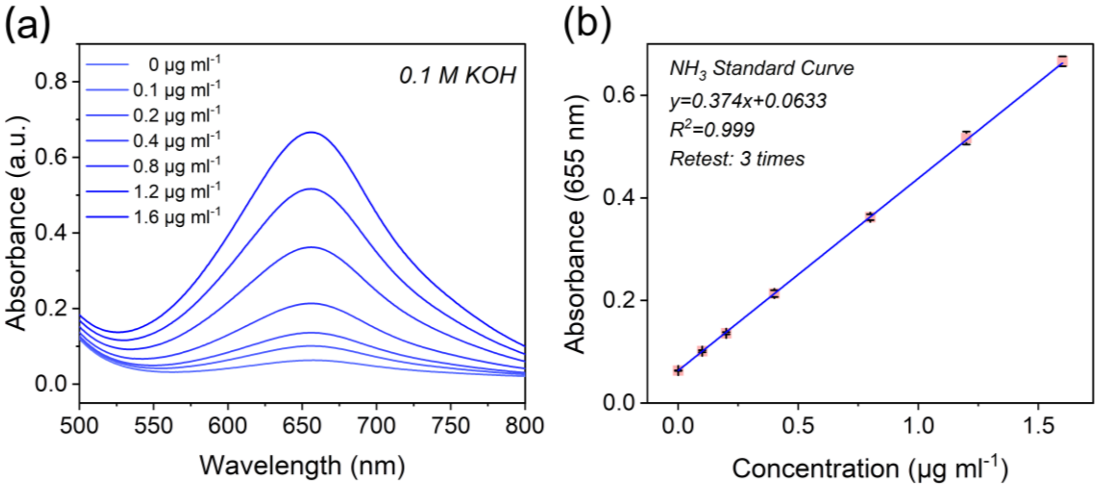

Figure S8. (a) The UV-vis absorption spectra and (b) corresponding calibration curve for the colorimetric NH_3 assay using the indophenol blue method in 0.1 M KOH. The error bars correspond to the standard deviations of measurements over three separately prepared samples under the same conditions.

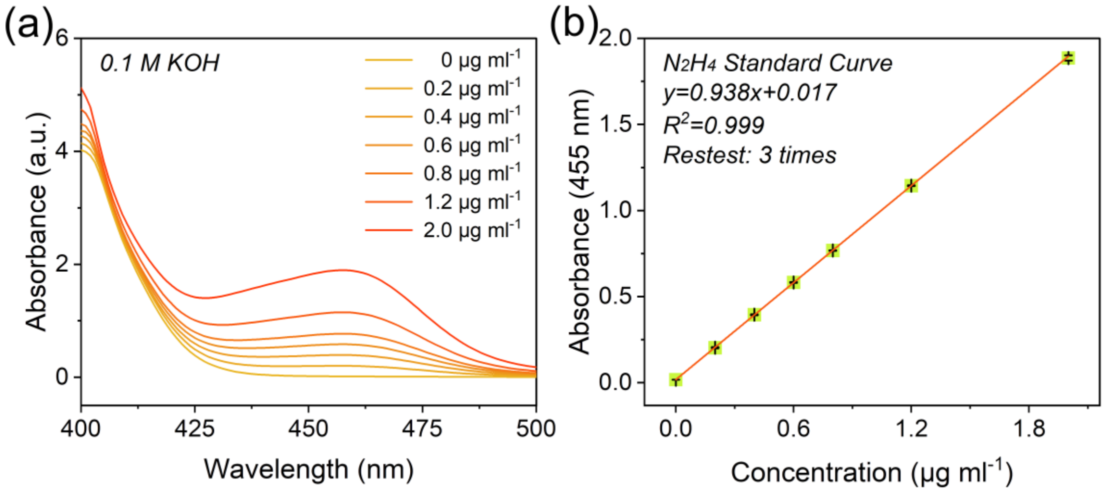

Figure S9. (a) The UV-vis absorption spectra and (b) corresponding calibration curve for the colorimetric N_2H_4 assay using the Watt and Chrisp method in 0.1 M KOH. The error bars correspond to the standard deviations of measurements over three separately prepared samples under the same conditions.

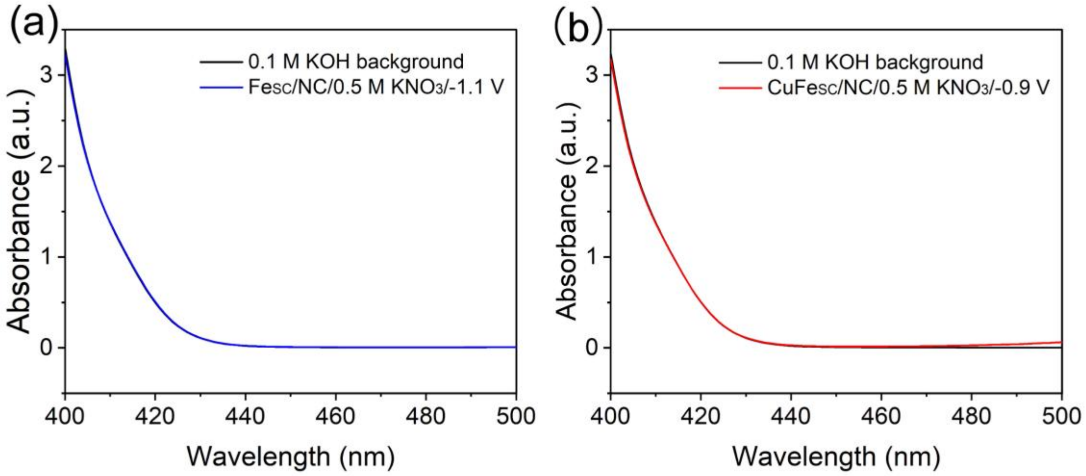

Figure S10. The UV-vis absorption spectra of the reaction electrolyte using the Watt and Chrisp method for (a) Fe_{SC}/NC and (b) $CuFe_{SC}$/NC.

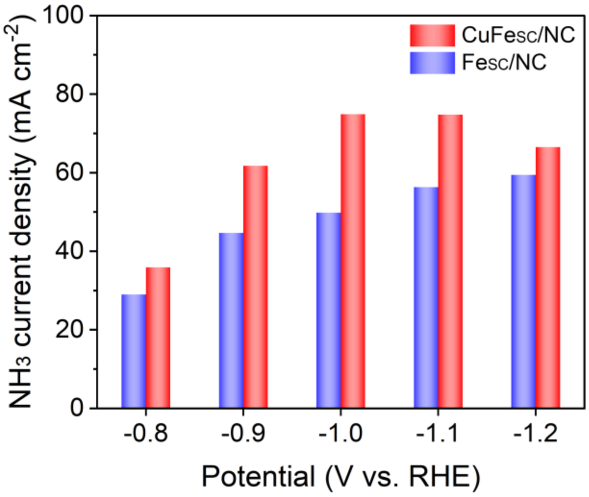

Figure S11. The NH_3 partial current density of Fe_{SC}/NC and $CuFe_{SC}$/NC.

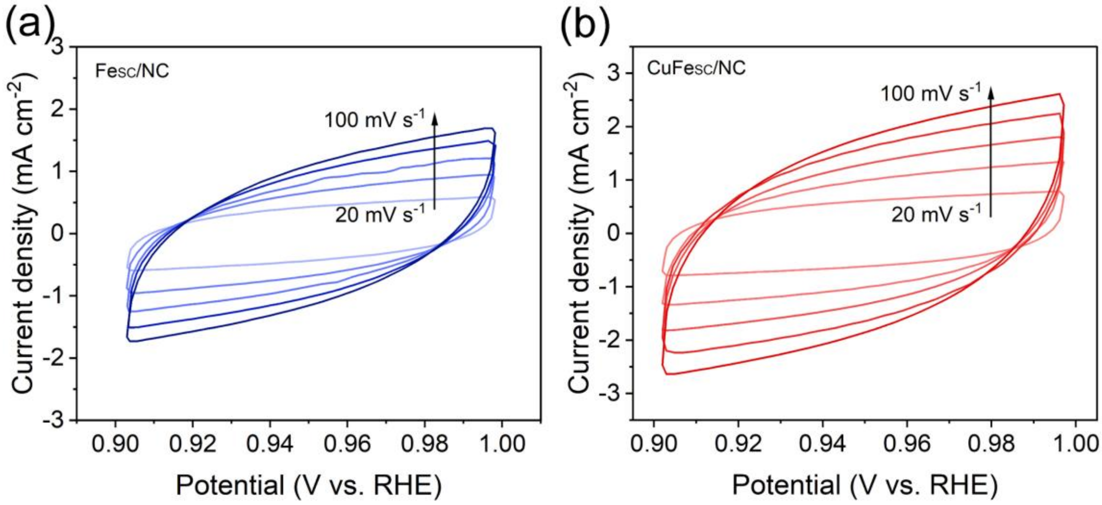

Figure S12. Cyclic voltammetry curves of (a) Fe_{SC}/NC and (b) $CuFe_{SC}$/NC catalysts measured at different scan rates from 20 to 100 mV s^{-1}.

Table S2. Comparison of NO_3RR activity for $CuFe_{SC}/NC$ with other reported electrocatalysts.

Catalyst	**Electrolyte**	**NH_3 yield rate (mmol h^{-1} mg^{-1})**	**Faradaic efficiency (%)**	**NH_3 partial current (mA cm^{-2})**	**Ref.**
$CuFe_{CS}/NC$	0.1 M KOH + 0.5 M KNO_3	10.51	93.28	211.9	This work
Ru_{SA}-NC	1.0 M KOH + 0.5 M KNO_3	2.76	72.80	125	1
Fe SAC	0.1 M K_2SO_4 + 0.5 M KNO_3	1.18	75.00	100	2
Fe_1/NC-900	0.1 M K_2SO_4 + 0.5 M KNO_3	1.10	86.00	50	3
FeN_2O_2 SAC	0.1 M K_2SO_4 + 0.5 M KNO_3	2.706	92	200	4
NJUZ-2	0.5 M Na_2SO_4 + 0.5 M KNO_3	0.23	91	70	5
Strained Ru clusters	1.0 M KNO_3 + 1.0 M KOH	5.56	42.00	120	6
Cu-N_4	1.0 M KNO_3 + 0.1 M KOH	12.50	84.70	50	7

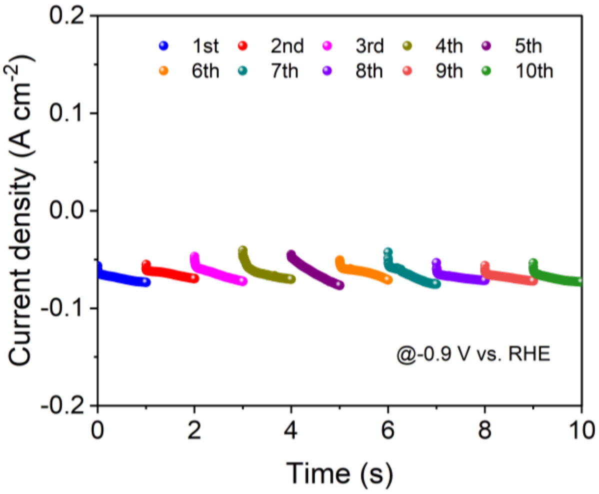

Figure S13. Chronoamperometry results of durability test of $CuFe_{SC}$/NC.

Reference

1. Z. Ke, D. He, X. Yan, W. Hu, N. Williams, H. Kang, X. Pan, J. Huang, J. Gu and X. Xu, *ACS Nano*, 2023, **17**, 3483.

2. Z. Wu, M. Karamad, X. Yong, Q. Huang, D. A. Cullen, P. Zhu, C. Xia, Q. Xiao, M. Shakouri, F. Chen, J. Y. Kim, Y. Xia, K. Heck, Y. Hu, M. S. Wong, Q. Li, I. Gates, S. Siahrostami and H. Wang, *Nat. Commun.*, 2021, **12**, 2870.

3. L. Liu, T. Xiao, H. Fu, Z. Chen, X. Qu and S. Zheng, *Appl. Catal. B-Environ. Energy*, 2023, **323**, 122181.

4. W. D. Zhang, H. Dong, L. Zhou, H. Xu, H. R. Wang, X. Yan, Y Jiang, J. Zhang and Z. G. Gu, *Appl. Catal. B-Environ. Energy*, 2022, **317**, 121750.

5. M. Wang, S. Li, Y. Gu, W. Xu, H. Wang, J. Sun, S. Chen, Z. Tie, J. L. Zuo, J. Ma, J. Su and J. Su, *J. Am. Chem. Soc.*, 2024, **146**, 20439-20448.

6. J. Li, G. Zhang, J. Yang, F. Quan, C. Mao, Y. Liu, B. Wang, F. Lei, L. Li, L. Xu, Y. Du, W. Hao, P. K. Wong, J. Wang, S. Dou, L. Zhang and J. C. Yu, *J. Am. Chem. Soc.*, 2020, **142**, 7036-7046.

7. J. Yang, H. Qi, A. Li, X. Liu, X. Yang, S. Zhang, Q. Zhao, Q. Jiang, Y. Su, L. Zhang, J. F. Li, Z. Q. Tian, W. Liu and A. Wang, *J. Am. Chem. Soc.*, 2022, **144**, 12062.